Effects of Different Microstructured Surfaces on the Osseointegration of CAD/CAM Zirconia Dental Implants: An Experimental Study in Rabbits

Qian Ding, DDS[1]/Rui Zhang, DDS[2]/Lei Zhang, DDS[1]/Yuchun Sun, DDS[3]/Qiufei Xie, PhD[1]

Purpose: To assess different microstructured surfaces created by sandblasting and acid etching in an effort to optimize the osseointegration performance of dental zirconia implants with an optimized surface. ***Materials and Methods:*** Sixty CAD/CAM zirconia implants were divided into four groups. The control group had no surface treatment after sintering. The other groups had three different types of surface modifications: sandblasting; sandblasting and etching with hydrofluoric acid; and sandblasting and etching with an experimental hot etching solution composed of methanol, 37% hydrochloric acid, and ferric chloride, heated to 100°C and applied for 60 minutes. Commercially available titanium implants with sandblasted and etched surfaces and identical dimensions were employed as a positive control. Surface micromorphologies of implants from the five groups were evaluated. The osseointegration performance of all the implants was assessed in adult New Zealand rabbits based on microcomputed tomography (micro-CT) and histologic analysis. ***Results:*** Sandblasting and acid etching with hot etching solution or hydrofluoric acid exhibited moderately rough surfaces with microstructures in both microscale and nanoscale. The sandblasting and etching with hydrofluoric acid group showed the highest surface roughness. Micro-CT revealed a significantly lower mean bone volume/total volume for the control group compared with the other four groups ($P < .05$). Among the groups, the sandblasting and hydrofluoric acid etching group was the highest, significantly higher than the titanium implant and sandblasting groups ($P < .05$). The sandblasting and etching with hot etching solution ($P = .006$) group also showed a significantly higher bone volume/total volume value than the titanium implant group. Histologic analysis revealed significantly higher bone-to-implant contact for implants with modified surfaces compared with a sintered surface ($P < .05$), and no significant difference was found with respect to the sandblasted and etched titanium implants. ***Conclusion:*** The microstructured surfaces created by sandblasting and acid etching show osseointegration comparable to that of commonly used titanium implants. *Int J Oral Maxillofac Implants 2020;35:1113–1121. doi: 10.11607/jomi.8207*

Keywords: dental implants, microstructure, osseointegration, surface topography, zirconia

[1]Department of Prosthodontics, Peking University School and Hospital of Stomatology, Beijing, China.
[2]Department of Prosthodontics, Stomatology Center, Peking University Shenzhen Hospital, Shenzhen, Guangdong, China.
[3]Center of Digital Dentistry, Peking University School and Hospital of Stomatology; National Engineering Laboratory for Digital and Material Technology of Stomatology; Research Center of Engineering and Technology for Digital Dentistry, Ministry of Health, Beijing, China.

Correspondence to: Dr Lei Zhang, 22 South Street ZhongGuanCun, Haidian District, Department of Prosthodontics, Peking University School and Hospital of Stomatology, Beijing 100081, China. Fax: +86 (10)62093402. Email: drzhanglei@yeah.net

Dr Yuchun Sun, 22 South Street ZhongGuanCun, Haidian District, Center of Digital Dentistry, Peking University School and Hospital of Stomatology, Beijing 100081, China. Email: polarshining@163.com

Yttria-stabilized tetragonal zirconia polycrystal (Y-TZP) has become a promising material for dental implants in recent years. Zirconia shows high chemical resistance and fracture toughness (7 to 10 MPa/m), reliable flexural strength (900 to 1,200 MPa), and decreased bacterial biofilm formation compared with titanium.[1–3] In addition, it has an esthetic advantage to a certain extent, especially in the anterior of the maxilla. Y-TZP has the potential to be an effective implant material alternative to titanium.[4,5] Since it is appropriate for computer-aided manufacturing (CAM), customized zirconia implants can be designed and fabricated using the CAD/CAM technique according to the characteristics of the individual patient's hard and soft tissues.

Surface microtopography was reported to have a major influence on both titanium and zirconia implant osseointegration, with increased surface roughness leading to greater bone apposition[6–8] and decreased

healing time.[9,10] The superior osseointegration of zirconia implants with different modified surfaces compared with machined, unmodified surfaces has been confirmed in experimental studies using rabbit models.[11,12] Nevertheless, the optimal surface modification or surface microtopography for zirconia implants has not yet been determined. The most common surface treatment of zirconia implants in previous studies is sandblasting with airborne particles.[13,14] Nanoscale surface modifications using acid etching in addition to sandblasting has been presented as an effective method that affects the cellular activities of osteoblasts and promotes osseointegration.[15,16] However, while this process has been widely applied to titanium,[9] it has rarely been tested in vivo for zirconia implants.[17]

A biomechanical study[18] and a histologic study[19] found that zirconia implants treated with hydrofluoric acid showed enhanced osseointegration, resulting in removal torque and bone-to-implant contact values equivalent to those of sandblasted and acid-etched titanium implants. Flamant et al[20] reported that hydrofluoric acid etching induced roughness gradients at both the microscale and nanoscale, affecting the mesenchymal stem cell morphology on the zirconia surface. The combination of sandblasting and hydrofluoric acid etching could also enhance the proliferation and differentiation of preosteoblasts.[21]

Experimental hot etching solution was first used to etch the wings of etched and bonded fixed dental prostheses to roughen the surfaces and enhance retention.[22] It was composed of methanol, 37% hydrochloric acid, and ferric chloride, then heated to 100°C. The mechanism is related to the chemical dissolution of the grain structure[23] and removal of the less-arranged, higher-energy atoms on the zirconia surface. Casucci et al[24] reported that experimental hot etching solution could be used to significantly modify the zirconia surface on the nanoscale. This procedure has the potential to improve the surface nanoroughness of zirconia implants. However, it has not been used in the surface treatment of zirconia implants. Accordingly, hydrofluoric acid and experimental hot etching solution were selected as surface modification methods in this study, and how they affect the nanoscale surface topography of zirconia was analyzed.

Based on the above discussion, the specific aims of this study were to determine the optimized surface microstructure design and to optimize the osseointegration performance of zirconia implants in a rabbit model. The effects of different microstructured surfaces with both microscale and nanoscale topography created by sandblasting and acid etching on the osseointegration of zirconia dental implants were investigated, compared with a well-established titanium implant. The null hypothesis was that microstructured surfaces have no influence on the osseointegration of zirconia implants.

MATERIALS AND METHODS

Implants

Cylindrical screw-type implants were designed using 3D computer-aided design (CAD) software (CATIA V5R19, Dassault Systèmes; Geomagic Studio 12.0, Geomagic). Based on the CAM technique, 60 zirconia implants were fabricated by cutting 3Y-TZP milling blocks (Wieland) and final sintering (Zenotec Fire P1, Wieland). All implants had a diameter of 3.75 mm, an intraosseous length of 6 mm, and spiral threads with pitch = 1.2 mm and depth = 0.5 mm.

Fifteen commercially available titanium implants (BEGO Implant Systems) with blasted and etched TiPurePlus surfaces and identical dimensions (3.75 × 8 mm) were employed as the positive control group (BEGO titanium implant group).

Surface Treatments and Topography Analysis

The following types of surface treatments were used for zirconia implants:

- Sintering (control group).
- Sandblasting: sandblasted with 110-μm Al_2O_3 particles at 0.45 MPa (Ovaljet HiBlaster, SHOFU).
- Sandblasting and etching with a hot solution: Following the protocol reported by Casucci et al,[24] 100-mL solution composed of 80 mL methanol, 20 mL 37% hydrochloric acid, and 0.2 g ferric chloride was heated to 100°C and etched for 60 minutes.
- Sandblasting and hydrofluoric acid etching: Etched in 40% hydrofluoric acid solution for 60 minutes at ambient temperature.[25]

After surface treatments, all zirconia implants were immersed in acetone, absolute alcohol, and deionized water sequentially and washed in an ultrasonic cleaner for 20 minutes each. After drying for 24 hours,[26] all implants were sterilized at high temperature and high pressure before surgery.

Scanning electron microscopy (SEM; JEOL, JSM-6010LA) was used to observe the surface topographies of the implants. The surface roughness was evaluated using a 3D laser microscope (VK-9700K, Keyence) scanning over an area of 700 × 500 μm between the screw threads to calculate roughness parameters (Ra, Rq, and Rz).

Animals and Surgical Procedures

The study protocol was approved by the Ethics Committee of Peking University, China (LA2019061). A total of 19 male New Zealand White rabbits (weight 2.5 to 3 kg) were used. A preoperative antibiotic (penicillin, 480 mg) was administered intramuscularly. All animals were anesthetized by injecting phenobarbital sodium

Fig 1 Radiographs of two CAD/CAM zirconia implants placed in the *(a)* femoral condyles and *(b)* proximal tibial metaphysis.
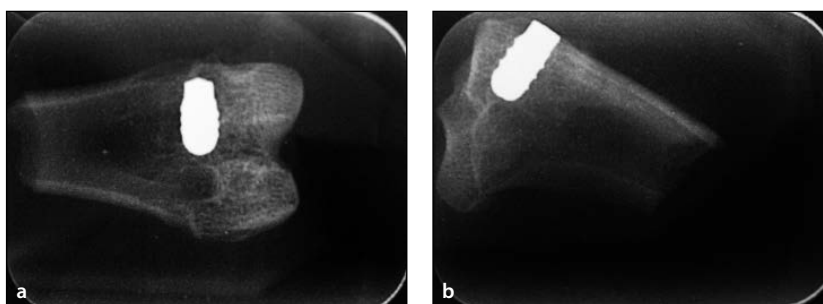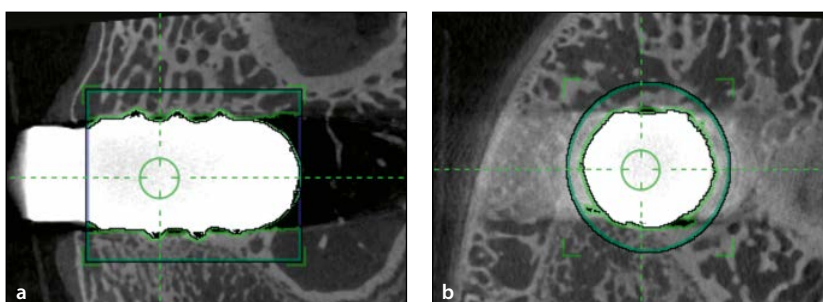

Fig 2 Micro-CT images showing cross sections of a CAD/CAM zirconia implant in *(a)* sagittal plane and *(b)* horizontal plane. The green solid line marks the region of interest. The CT value for the black area at the bottom of the implant is less than −1,000. This area was excluded from the region of interest because of the presence of significant artifacts.

(30 mg/kg) through the ear vein. Supplemental anesthetics were prepared as needed during the surgery. The bilateral distal femoral condyles and proximal tibial metaphyses were used as experimental sites (Fig 1). After surgical draping, the diaphysis was exposed via a skin incision and a blunt dissection of the muscles to allow elevation of the periosteum. BEGO System drills (BEGO Implant Systems) were used to prepare the implant site under irrigation with 4°C sterile saline.

One implant was placed in each experimental site of each rabbit. With a total of 75 implants, there would be a rabbit with the insertion of only three implants. In order to make the same healing potency for all animals, a zirconia cylinder specimen with a sintered surface was added. The four implants in each rabbit from different groups were numbered and randomly allocated to sites using the website http://www.randomization.com. The implants were then inserted with a torque of 10 to 15 Ncm and achieved primary stability. All zirconia implants were inserted with the hexagonal coronal portion superior to the cortex. Titanium implants were placed by matching the implant shoulder to the cortex. After the insertion of the implants, the fascia and skin were sutured in separate layers with resorbable sutures (Vicryl 5-0, Ethicon). After surgery, the animals were closely observed for any abnormal signs, such as wound dehiscence or infection. Perioperative antibiosis was performed with a 3-day course of a wide-spectrum antibiotic (penicillin, 480 mg/d, intramuscular).

Retrieval of Specimens

At 6 weeks after surgery, the animals were sacrificed by intravenous overdoses of lidocaine at 2%. The implants were surgically exposed, and bone blocks containing the implants and surrounding tissue were dissected and stored in 10% formalin at 4°C for microcomputed tomography (micro-CT) and histologic evaluations.

Micro-CT Analysis

The specimens were scanned in a micro-CT machine (MM CT, Inveon Acquisition Workplace, SIEMENS) to analyze 3D bone formation around the implants. The slice resolution was 18 µm. A total of 1,024 micro-CT slices for each specimen were imaged at an x-ray energy level of 80 kV and a current of 500 µA. The integration time was 400 ms, and the total scanning time per specimen was approximately 27 minutes.

COBRA_Exxim software was used for 3D image reconstruction, and the reconstructed images were imported into the Inveon Research Workplace (SIEMENS) for evaluation. The region of interest was defined as a 500-µm-wide zone around the implant surface that began with the most apical slice containing the implant and extended up to the original implantation level[27] (Fig 2). To reduce the influence of artifacts, the black area at the bottom of each implant was excluded from the region of interest because of the significant artifacts presented in this area. The grayscale values for the bone and implant were determined as thresholds by comparing the original grayscale scan to different threshold levels of the complete slices and determining the threshold values for the mineralized bone and implant. All specimens had similar threshold levels for the bone and implant, which had no overlap and permitted clear distinction.[28] The minimum threshold in micro-CT analysis was set to −1,000 (the grayscale value

of air). Voxels with grayscale values above and below these values could then be categorized as background, implant, or mineralized bone, respectively. Threshold determination was repeated to evaluate intraexaminer repeatability.

Subsequently, the bone morphology parameters and bone mineral density were calculated in the region of interest for each specimen. The outcome variables included the bone volume/total volume (ie, the percentage of bone volume in the region of interest), trabecular thickness, trabecular number, trabecular spacing, and bone mineral density.

Histologic Evaluation

After being submerged in 10% formalin solution for at least 24 hours, the specimens were washed with running water and dehydrated in a graded series of ethanol solutions. The dehydrated specimens were embedded in polymethyl methacrylate without decalcification according to standard procedures and sectioned in the frontal plane through the middle of the implant to obtain sections with a thickness of 200 μm. The sections were ground, polished to a uniform thickness of 60 μm, and surface-stained with toluidine blue.

Computer-based histomorphometric analysis was performed under a light microscope equipped with a high-resolution camera at a magnification of 40×. Bone morphometry data were analyzed using a software program (BIOQUANT OSTEO Bone Biology Research System, v13.2.6, BIOQUANT Image Analysis Corporation). The bone-to-implant contact and bone area (equivalent to 2D bone volume/total volume) were measured in the region of interest (also defined as a 500-μm-wide zone around the implant surface). The lengths of all regions with direct bone-to-implant contact in the region of interest were measured, and their sum was divided by the total length of the implant perimeter in the area to obtain the percentage of bone-to-implant contact. All the sections were numbered, and the investigator who conducted micro-CT and histologic evaluations was blind to the grouping of each zirconia implant.

Statistical Analysis

The statistical analysis was performed using SPSS 22.0 statistical software (SPSS, IBM). Mean values and SDs of all outcome variables were calculated for each group. All values are expressed as mean ± SD. The normal distribution and homogeneity of variance were tested using two-tailed analysis. When variances were homogenous and observed values were distributed normally, one-way analysis of variance and least significant difference tests (for multiple comparisons) were applied to detect differences between means of the five groups. Otherwise, a nonparametric analysis of the Kruskal-Wallis H test was performed. $P < .05$ and $P < .01$ were considered statistically significant and highly significant, respectively.

RESULTS

Surface Micromorphology and Surface Roughness of Implants

The SEM images in Fig 3 show that the implant surfaces in the control group were relatively flat, with flaws and microcracks created during the CAM process. In the sandblasting group, the implant surfaces exhibited a microrough topography including peaks and valleys with sharp margins. Sandblasting and etching with hot etching solution surfaces became smoother with microscale grooves and irregular nanoscale pores. In contrast, the sandblasting and hydrofluoric acid etching surfaces appeared with granular textures and etch pits, resulting in both nanoroughness and microroughness. The titanium implant surface exhibited typical features of a sandblasted and etched surface with multilevel pores. Table 1 shows the surface roughness levels. The highest Ra value was with the sandblasting and hydrofluoric acid etching group, and the lowest was the control group, with significant differences with the other four groups ($P < .01$). Ra values of the sandblasting, sandblasting and etching with hot etching solution, and sandblasting and hydrofluoric acid etching groups were not significantly different from that of the titanium implant group ($P > .05$).

General Observations

Two implants were excluded from the results: one implant in the sandblasting group developed a peri-implant infection, and one in the sandblasting and hydrofluoric acid etching group appeared to be enclosed by fibrous connective tissue instead of osseointegration. The remaining 73 implants were placed in the correct submerged position, and no signs of infection or defluvium were observed. Routine clinical inspections showed uneventful postoperative healing. After 6 weeks of healing, all the remaining implants in the bone blocks were immobile, suggesting osseointegration. Around the implant head, the hexagonal coronal portions of 39 implants were partly or fully covered with newly formed bone (Fig 1), indicating the good biocompatibility of zirconia.

Micro-CT Analysis

The results of 3D bone morphometric analysis are presented in Table 2 and Fig 4. Compared with the control group, significantly increased bone volume/total volume and bone mineral density values were revealed in the sandblasting group ($P < .01$), sandblasting and etching with hot etching solution group, and sandblasting
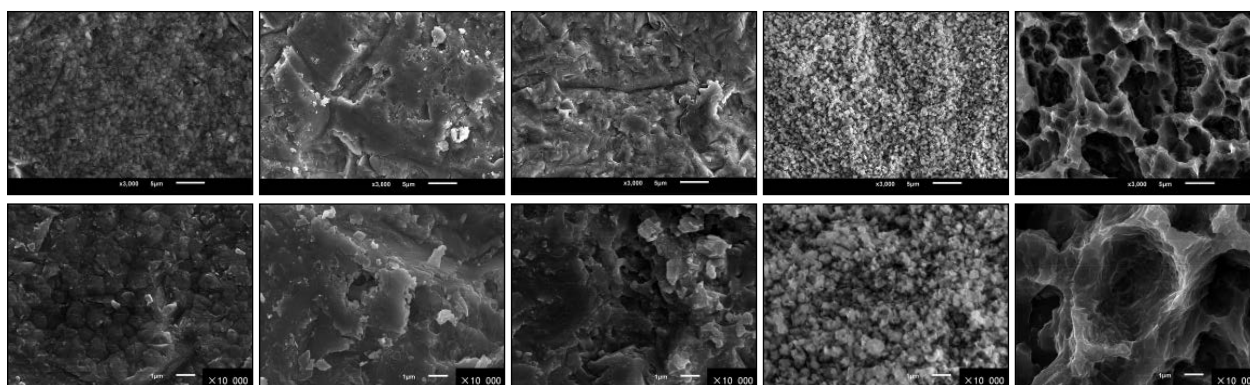
Fig 3 SEM images showing the surface microtopographies of zirconia and titanium implants from five groups. CTRL = control group; SB = sandblasting group; SB-ST = sandblasting and etching with an experimental hot etching solution; SB-HF = sandblasting and hydrofluoric acid etching; BEGO = BEGO titanium implants.

Table 1 Mean Surface Topographic Parameters of the Implants Used in the Study (n = 3)			
Implants	Ra (μm)	Rq (μm)	Rz (μm)
Control	0.674 ± 0.034	0.857 ± 0.039	6.806 ± 0.425
Sandblasting	1.316 ± 0.089	1.615 ± 0.104	10.815 ± 0.484
Sandblasting and etching with hot etching solution	1.508 ± 0.056	1.844 ± 0.078	12.825 ± 0.951
Sandblasting and hydrofluoric acid etching	1.686 ± 0.168	2.062 ± 0.203	12.932 ± 1.146
BEGO titanium implants	1.544 ± 0.065	1.955 ± 0.081	12.567 ± 1.476

and hydrofluoric acid etching group ($P < .001$); for the titanium implant group, the difference was only significant for bone volume/total volume ($P = .027$). The sandblasting and etching with hot etching solution ($P = .006$) and sandblasting and hydrofluoric acid etching ($P = .001$) groups showed significantly greater bone volume/total volume values than the titanium implant group, while only the sandblasting and hydrofluoric acid etching group exhibited a significantly higher bone volume/total volume ($P = .028$) and bone mineral density ($P = .001$) compared with the sandblasting group. No significant difference was observed between the bone volume/total volume and bone mineral density values of the sandblasting and sandblasting and etching with hot etching solution groups. The comparison between the sandblasting and titanium implant groups also showed no significant difference.

Histologic Analysis

Six weeks after implant placement, successful osseointegration was observed in both the zirconia and titanium implants. At the interfaces with direct bone-to-implant contact, no gaps or fibrous tissues were found, and new bone formation and remodeling were observed. In the control group, small areas of bone-to-implant contact were interrupted by portions of soft tissue, and nonmineralized tissue layers were observed around the implant surfaces in most cases. In other groups, the bone-to-implant contact was more consolidated, and some areas exhibited more mature lamellar bone around the implant surfaces (Fig 5).

As shown in Table 3 and Fig 4, the bone-to-implant contact values of the sandblasting, sandblasting and etching with hot etching solution, and sandblasting and hydrofluoric acid etching groups were significantly higher than that of the control group ($P < .05$) but did not significantly differ from that of the titanium implant group ($P > .05$). The values did not differ significantly among the sandblasting, sandblasting and etching with hot etching solution, and sandblasting and hydrofluoric acid etching groups. However, the bone area values of the sandblasting and etching with hot etching solution group ($P = .011$) and sandblasting and hydrofluoric acid etching ($P = .045$) groups were significantly higher than that of the titanium implant group.

DISCUSSION

The zirconia implant surfaces with microstructures created by sandblasting alone or sandblasting and etching in this study demonstrated good osseointegration

Table 2 Results of Micro-CT Bone Morphometry Analysis (Mean ± SD)

Implants	Bone volume/total volume (%)	Trabecular thickness (mm)	Trabecular number (1/mm)	Trabecular spacing (mm)	Bone mineral density (mg/cm³)
Control	46.10 ± 4.70	0.092 ± 0.016	5.07 ± 0.66	0.11 ± 0.015	1,378.59 ± 97.48
Sandblasting	54.72 ± 6.14	0.11 ± 0.028	5.19 ± 1.01	0.091 ± 0.023	1,529.12 ± 66.48
Sandblasting and etching with hot etching solution	58.81 ± 5.86	0.12 ± 0.014	4.87 ± 0.62	0.087 ± 0.021	1,507.54 ± 73.89
Sandblasting and hydrofluoric acid etching	60.30 ± 7.87	0.141 ± 0.051	4.74 ± 1.45	0.092 ± 0.036	1,998.83 ± 132.12
BEGO titanium implants	51.73 ± 8.42	0.10 ± 0.016	5.20 ± 0.74	0.095 ± 0.024	1,446.98 ± 44.42

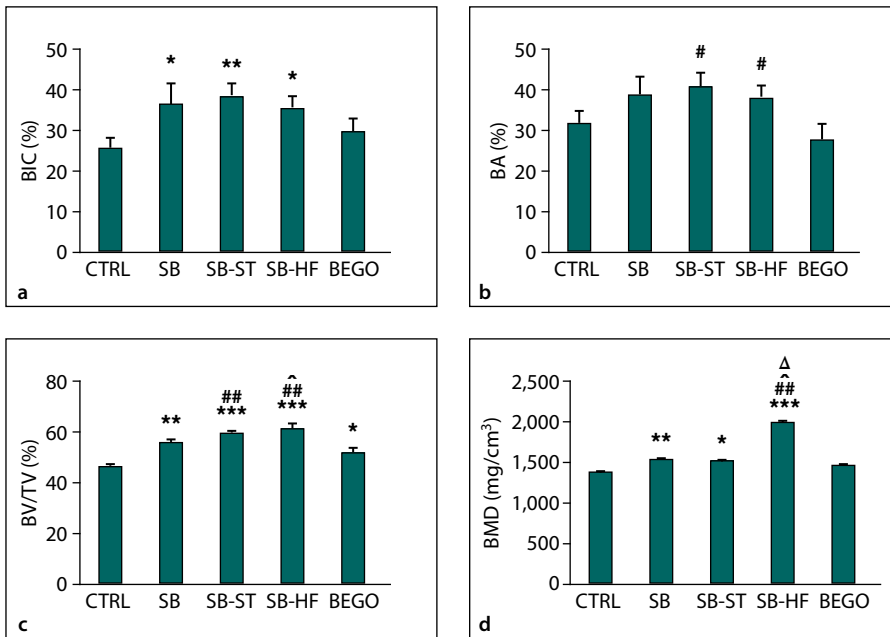n = 15 for all groups, except sandblasting and sandblasting and hydrofluoric acid etching, where n = 14.

Fig 4 Bar graphs showing the results of *(a)* bone-to-implant contact (BIC), *(b)* bone area (BA), *(c)* bone volume/total volume (BV/TV), and *(d)* bone mineral density (BMD) values after 6 weeks of implantation. CTRL = control group; SB = sandblasting group; SB-ST = sandblasting and etching with an experimental hot etching solution; SB-HF = sandblasting and hydrofluoric acid etching; BEGO = BEGO titanium implants. n = 15 for all groups, except SB and SB-HF, where n = 14. Statistically significant differences are indicated as follows: *P < .05, **P < .01, ***P < .001 compared with the CTRL group; #P < .05, ##P < .01, ###P < .001 compared with the BEGO group; ^P < .05 compared with the SB group; △P < .05 compared with the SB-ST group.
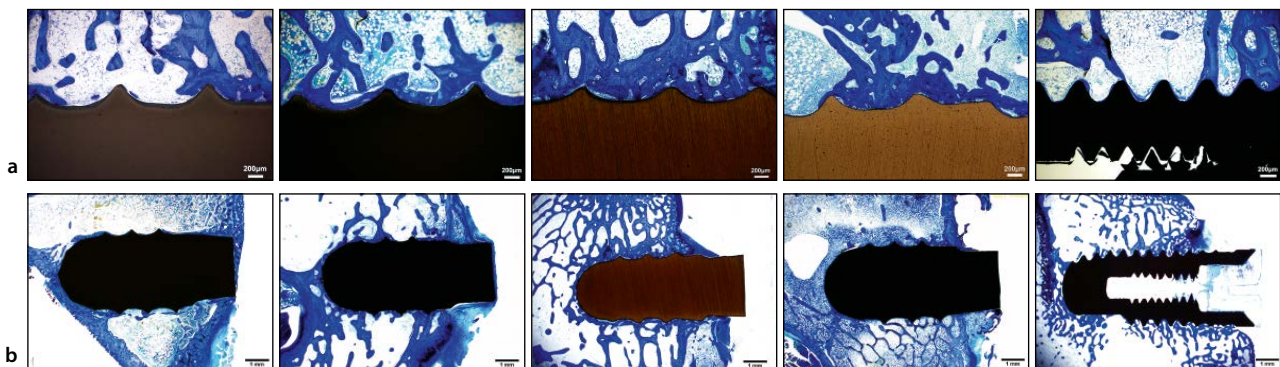

Fig 5 Light micrographs showing the degree of bone-to-implant contact of the zirconia and titanium implants at 6 weeks after implant placement (*[a]* magnification = 40×; *[b]* magnification = 12.5×). CTRL = control group; SB = sandblasting group; SB-ST = sandblasting and etching with an experimental hot etching solution; SB-HF = sandblasting and hydrofluoric acid etching; BEGO = BEGO titanium implants.

Table 3 Histologic Analysis Results of the Implant Groups After 6 Weeks of Healing Time (Mean ± SD)

Implants	Bone-to-implant contact (%)	Bone area (%)
Control	27.92 ± 9.46	33.38 ± 10.51
Sandblasting	36.39 ± 15.33	37.10 ± 16.96
Sandblasting and etching with hot etching solution	39.23 ± 9.74	40.64 ± 12.95
Sandblasting and hydrofluoric acid etching	35.34 ± 12.83	38.07 ± 12.21
BEGO titanium implants	29.87 ± 11.14	27.80 ± 12.33

n = 15 for all groups, except sandblasting and sandblasting and hydrofluoric acid etching, where n = 14.

equivalent to or better than that achieved by sandblasted and etched titanium implant surfaces. Previous animal and clinical studies also revealed the successful osseointegration of surface-modified zirconia implants, with osseointegration comparable to that of well-established titanium implants.[29–31]

This study took the lead in investigating the osseointegration of four different surface-treated zirconia implants, and two different acid etching methods were used to create nanoscale surface topography on the zirconia surface, with experimental hot etching solution first used in zirconia implant surface modification. Overall, this study demonstrated that microstructured surfaces can improve the osseointegration of zirconia implants. Thus, the null hypothesis must be rejected. However, compared with sandblasted surfaces, the nanostructures created by acid etching showed no significant improvement in the bone-to-implant contact values of the zirconia implants but showed a significant increase in peri-implant bone area, while the sandblasted and hydrofluoric acid-etched surfaces showed significantly higher bone volume/total volume and bone mineral density values compared with the sandblasted surfaces in micro-CT analysis. Therefore, the nanotopography created by acid etching, especially hydrofluoric acid etching, may play a role in improving peri-implant bone formation.

Al_2O_3 particles with granule sizes ranging from 105 to 250 μm are the most commonly used particles for sandblasting zirconia implant surfaces.[14,32] However, the biologic effects of surface contamination by residual Al_2O_3 particles remain controversial.[33,34] In addition to removing contamination resulting from sandblasting, surface modification by additional acid etching adds nanoscale topography to the microtopography of zirconia implants. The advantages of surface nanotopography were reported to include an increase in the total surface contact area of the implant, better mimicry of cellular environments, and improved cell behavior and cell interactions at surfaces compared with conventional surface topography.[35] A systematic review[17] reported that zirconia implants with acid-etched surfaces

showed significantly higher bone-to-implant contact than titanium implants. Also, acid-etched zirconia implants may serve as a possible alternative for successful osseointegration.

In this study, additional etching with either hot etching solution or hydrofluoric acid created nanoroughness on the zirconia surface. However, neither type of etching led to a significant improvement in bone-to-implant contact compared with the sandblasted implants. The differences between the findings of this study and past works may be related to the use of different sandblasting and etching techniques, leading to different surface micro- and nanotopographies. Another explanation may be the healing time considered herein; this study only evaluated a 6-week healing period in rabbits, which was selected to coincide with the timespan required for complete bone healing in humans.[36] Therefore, early peri-implant bone responses based on different surface microstructures were not investigated, which is a limitation of this study. Nevertheless, the present study focused on the evaluation at the time point of 6 weeks, using sufficient samples and five groups of implants. Further research will focus on the effects of surface micro- and nanotopography on early peri-implant bone response and initial biomechanical performance of zirconia implants.

Nanostructures have been shown to elicit complex initial gene responses that favor healing at the bone-implant interface.[37] Schliephake et al[14] reported that the bone-to-implant contact value showed no significant difference between zirconia implants with sandblasted surfaces and sandblasted and etched surfaces in minipigs at both 4 weeks and 3 months after implantation time. Significantly higher removal torque was shown in sandblasted and etched zirconia implants compared with the sandblasted implants at 4 weeks after implantation; however, this difference disappeared after 3 months. Halldin et al[38] investigated the effects of different surface microstructures created by oxalic acid and hydrofluoric acid etching on the osseointegration of titanium implants.

They concluded that alteration of the nanostructure might improve the initial biomechanical performance, whereas the surface interlocking capacity seemed to play a more important role after longer healing times. This suggests that for long healing times, the surface microtopography is the main factor affecting the degree of implant osseointegration.

Histologic analysis is limited by the fact that it is based on one or a few sections cut from the specimen. Micro-CT has the potential to overcome this limitation; micro-CT is less time consuming than histologic analysis, is nondestructive, and permits 3D analysis. Micro-CT has been used to evaluate peri-implant bone structure in many studies,[27,39] and this method has been validated by histologic findings.[28,40] The investigation of trabecular bone around titanium implants using micro-CT was highly reliable for the determination of trabecular bone parameters.[41] The only disadvantage of micro-CT was the inaccurate measurement of direct bone-to-implant contact areas due to inevitable artifacts. Therefore, the combined use of micro-CT and histologic examinations in this study was a holistic and reliable strategy to evaluate implant osseointegration.

However, the bone volume/total volume values determined using micro-CT were significantly higher than the bone area values (ie, 2D bone volume/total volume) assessed using histologic analysis in this study ($P < .01$). One reason was that measurement variations caused by the orientation of the section around the center line of the implant were reported to be approximately 30%.[42] Another important reason is the influence of artifacts on micro-CT data, which could hinder reliable discrimination between bone and soft tissue at the implant interface.[43] This may have resulted in the overestimation of bone volume/total volume and bone mineral density based on micro-CT.

CONCLUSIONS

Within the limitations of this animal study, it is concluded that compared with sintered or sandblasted zirconia implants, implants treated by sandblasting and acid etching with hot etching solution or hydrofluoric acid exhibited moderately rough surfaces (Ra = 1 to 2 μm) with microstructures in both microscale and nanoscale, resulting in a significantly higher degree of osseointegration that is equivalent to or better than that achieved by the well-established titanium implants. When considering long healing times, the surface microtopography is the main factor affecting the degree of implant osseointegration. The nanotopography created by acid etching, especially hydrofluoric acid etching, may play a role in improving peri-implant bone formation.

REFERENCES

1. Özkurt Z, Kazazoğlu E. Zirconia dental implants: A literature review. J Oral Implantol 2011;37:367–376.
2. Piconi C, Maccauro G. Zirconia as a ceramic biomaterial. Biomaterials 1999;20:1–25.
3. Scarano A, Piattelli A, Polimeni A, Di Iorio D, Carinci F. Bacterial adhesion on commercially pure titanium and anatase-coated titanium healing screws: An in vivo human study. J Periodontol 2010;81:1466–1471.
4. Oliva J, Oliva X, Oliva JD. Five-year success rate of 831 consecutively placed zirconia dental implants in humans: A comparison of three different rough surfaces. Int J Oral Maxillofac Implants 2010;25:336–344.
5. Andreiotelli M, Wenz HJ, Kohal RJ. Are ceramic implants a viable alternative to titanium implants? A systematic literature review. Clin Oral Implants Res 2009;20(suppl 4):32–47.
6. Gahlert M, Roehling S, Sprecher CM, Kniha H, Milz S, Bormann K. In vivo performance of zirconia and titanium implants: A histomorphometric study in mini pig maxillae. Clin Oral Implants Res 2012;23:281–286.
7. Pieralli S, Kohal RJ, Lopez Hernandez E, Doerken S, Spies BC. Osseointegration of zirconia dental implants in animal investigations: A systematic review and meta-analysis. Dent Mater 2018;34:171–182.
8. Mihatovic I, Golubovic V, Becker J, Schwarz F. Bone tissue response to experimental zirconia implants. Clin Oral Investig 2017;21:523–532.
9. Cochran DL, Buser D, ten Bruggenkate CM, et al. The use of reduced healing times on ITI implants with a sandblasted and acid-etched (SLA) surface: Early results from clinical trials on ITI SLA implants. Clin Oral Implants Res 2002;13:144–153.
10. Buser D, Broggini N, Wieland M, et al. Enhanced bone apposition to a chemically modified SLA titanium surface. J Dent Res 2004;83:529–533.
11. Sennerby L, Dasmah A, Larsson B, Iverhed M. Bone tissue responses to surface-modified zirconia implants: A histomorphometric and removal torque study in the rabbit. Clin Implant Dent Relat Res 2005;7(suppl 1):s13–s20.
12. Aboushelib MN, Salem NA, Taleb AL, El Moniem MN. Influence of surface nano-roughness on osseointegration of zirconia implants in rabbit femur heads using selective infiltration etching technique. J Oral Implantol 2013;39:583–590.
13. Manzano G, Herrero LR, Montero J. Comparison of clinical performance of zirconia implants and titanium implants in animal models: A systematic review. Int J Oral Maxillofac Implants 2014;29:311–320.
14. Schliephake H, Hefti T, Schlottig F, Gédet P, Staedt H. Mechanical anchorage and peri-implant bone formation of surface-modified zirconia in minipigs. J Clin Periodontol 2010;37:818–828.
15. Cheng B, Niu Q, Cui Y, Jiang W, Zhao Y, Kong L. Effects of different hierarchical hybrid micro/nanostructure surfaces on implant osseointegration. Clin Implant Dent Relat Res 2017;19:539–548.

16. Bergemann C, Duske K, Nebe JB, et al. Microstructured zirconia surfaces modulate osteogenic marker genes in human primary osteoblasts. J Mater Sci Mater Med 2015;26:5350.

17. Hafezeqoran A, Koodaryan R. Effect of zirconia dental implant surfaces on bone integration: A systematic review and meta-analysis. Biomed Res Int 2017;2017:9246721.

18. Gahlert M, Röhling S, Wieland M, Eichhorn S, Küchenhoff H, Kniha H. A comparison study of the osseointegration of zirconia and titanium dental implants. A biomechanical evaluation in the maxilla of pigs. Clin Implant Dent Relat Res 2010;12:297–305.

19. Gahlert M, Röhling S, Wieland M, Sprecher CM, Kniha H, Milz S. Osseointegration of zirconia and titanium dental implants: A histological and histomorphometrical study in the maxilla of pigs. Clin Oral Implants Res 2009;20:1247–1253.

20. Flamant Q, Stanciuc AM, Pavailler H, et al. Roughness gradients on zirconia for rapid screening of cell-surface interactions: Fabrication, characterization and application. J Biomed Mater Res A 2016;104:2502–2514.

21. Ito H, Sasaki H, Saito K, Honma S, Yajima Y, Yoshinari M. Response of osteoblast-like cells to zirconia with different surface topography. Dent Mater J 2013;32:122–129.

22. Ferrari M, Cagidiaco MC, Borracchini A, Bertelli E. Evaluation of a chemical etching solution for nickel-chromium-beryllium and chromium-cobalt alloys. J Prosthet Dent 1989;62:516–521.

23. Casucci A, Monticelli F, Goracci C, et al. Effect of surface pre-treatments on the zirconia ceramic-resin cement microtensile bond strength. Dent Mater 2011;27:1024–1030.

24. Casucci A, Osorio E, Osorio R, et al. Influence of different surface treatments on surface zirconia frameworks. J Dent 2009;37:891–897.

25. Flamant Q, Anglada M. Hydrofluoric acid etching of dental zirconia. Part 2: Effect on flexural strength and ageing behavior. J Eur Ceram 2016;36:135–145.

26. Li S, Ni J, Liu X, et al. Surface characteristics and biocompatibility of sandblasted and acid-etched titanium surface modified by ultraviolet irradiation: An in vitro study. J Biomed Mater Res B Appl Biomater 2012;100:1587–1598.

27. Anil S, Cuijpers VM, Preethanath RS, Aldosari AA, Jansen JA. Osseointegration of oral implants after delayed placement in rabbits: A microcomputed tomography and histomorphometric study. Int J Oral Maxillofac Implants 2013;28:1506–1511.

28. Vandeweghe S, Coelho PG, Vanhove C, Wennerberg A, Jimbo R. Utilizing micro-computed tomography to evaluate bone structure surrounding dental implants: A comparison with histomorphometry. J Biomed Mater Res B Appl Biomater 2013;101:1259–1266.

29. Hoffmann O, Angelov N, Zafiropoulos GG, Andreana S. Osseointegration of zirconia implants with different surface characteristics: An evaluation in rabbits. Int J Oral Maxillofac Implants 2012;27:352–358.

30. Manzano G, Herrero LR, Montero J. Comparison of clinical performance of zirconia implants and titanium implants in animal models: A systematic review. Int J Oral Maxillofac Implants 2014;29:311–320.

31. Kubasiewicz-Ross P, Hadzik J, Dominiak M. Osseointegration of zirconia implants with 3 varying surface textures and a titanium implant: A histological and micro-CT study. Adv Clin Exp Med 2018;27:1173–1179.

32. Janner SFM, Gahlert M, Bosshardt DD, et al. Bone response to functionally loaded, two-piece zirconia implants: A preclinical histometric study. Clin Oral Implants Res 2018;29:277–289.

33. Lacefield WR. Current status of ceramic coatings for dental implants. Implant Dent 1998;7:315–322.

34. Piattelli A, Degidi M, Paolantonio M, Mangano C, Scarano A. Residual aluminum oxide on the surface of titanium implants has no effect on osseointegration. Biomaterials 2003;24:4081–4089.

35. Mendonça G, Mendonça DB, Aragão FJ, Cooper LF. Advancing dental implant surface technology—From micron- to nanotopography. Biomaterials 2008;29:3822–3835.

36. Matos MA, Araújo FP, Paixão FB. Histomorphometric evaluation of bone healing in rabbit fibular osteotomy model without fixation. J Orthop Surg Res 2008;3:4.

37. Wazen RM, Kuroda S, Nishio C, Sellin K, Brunski JB, Nanci A. Gene expression profiling and histomorphometric analyses of the early bone healing response around nanotextured implants. Nanomedicine (Lond) 2013;8:1385–1395.

38. Halldin A, Jimbo R, Johansson CB, Gretzer C, Jacobsson M. Improved osseointegration and interlocking capacity with dual acid-treated implants: A rabbit study. Clin Oral Implants Res 2016;27:22–30.

39. Martins R, Cestari TM, Arantes RVN, et al. Osseointegration of zirconia and titanium implants in a rabbit tibiae model evaluated by microtomography, histomorphometry and fluorochrome labeling analyses. J Periodont Res 2018;53:210–221.

40. Park YS, Yi KY, Lee IS, Jung YC. Correlation between microtomography and histomorphometry for assessment of implant osseointegration. Clin Oral Implants Res 2005;16:156–160.

41. Stoppie N, van der Waerden JP, Jansen JA, Duyck J, Wevers M, Naert IE. Validation of microfocus computed tomography in the evaluation of bone implant specimens. Clin Implant Dent Relat Res 2005;7:87–94.

42. Sarve H, Lindblad J, Borgefors G, Johansson CB. Extracting 3D information on bone remodeling in the proximity of titanium implants in SRμCT image volumes. Comput Methods Programs Biomed 2011;102:25–34.

43. Liu PT, Pavlicek WP, Peter MB, Spangehl MJ, Roberts CC, Paden RG. Metal artifact reduction image reconstruction algorithm for CT of implanted metal orthopedic devices: A work in progress. Skeletal Radiol 2009;38:797–802.